

Article

# Broadband Coplanar Waveguide to Air-Filled Rectangular Waveguide Transition

Yuyu Zhao <sup>1</sup>, Jun Dong <sup>1,2,\*</sup> , Fan Yin <sup>1</sup>, Xinchun Fang <sup>1</sup> and Ke Xiao <sup>3</sup>

<sup>1</sup> College of Information Science and Engineering, Hunan Normal University, Changsha 410081, China; yyzhaocn@126.com (Y.Z.); yinfan7701@126.com (F.Y.); xinchunfang8825@126.com (X.F.)

<sup>2</sup> State Key Laboratory of Millimeter Waves, Southeast University, Nanjing 210096, China

<sup>3</sup> School of Electronic Science, National University of Defense Technology, Changsha 410073, China; xiaoke\_e@hotmail.com

\* Correspondence: jdongcn@outlook.com

**Abstract:** This article introduces a novel transition between coplanar waveguide (CPW) and air-filled rectangular waveguide (RWG). A rectangular radiator etched with a semi-elliptic slot is connected to the center conductor of CPW to realize the transition, which broadens the bandwidth. This direct transition does not require intermediate transition or air-bridges. Moreover, the planar circuit of the transition can be designed with high- and low-permittivity materials ( $\epsilon_r = 10.2$  and  $2.22$ ), which offer more benefits in both PCB and MMIC design. Two back-to-back transition prototypes at X-band are designed, fabricated and measured. The 15 dB fractional bandwidths are expanded to 44.7% and 47.6% respectively, which have been demonstrated in both of the transitions ( $\epsilon_r = 10.2$  and  $2.22$ ). The measurement results agree well with simulation results, which validate the feasibility of this design.

**Keywords:** CPW; rectangular waveguide; broadband transition



**Citation:** Zhao, Y.; Dong, J.; Yin, F.; Fang, X.; Xiao, K. Broadband Coplanar Waveguide to Air-Filled Rectangular Waveguide Transition. *Electronics* **2022**, *11*, 1057. <https://doi.org/10.3390/electronics11071057>

Academic Editor: Dal Ahn

Received: 23 February 2022

Accepted: 22 March 2022

Published: 28 March 2022

**Publisher's Note:** MDPI stays neutral with regard to jurisdictional claims in published maps and institutional affiliations.



**Copyright:** © 2022 by the authors. Licensee MDPI, Basel, Switzerland. This article is an open access article distributed under the terms and conditions of the Creative Commons Attribution (CC BY) license (<https://creativecommons.org/licenses/by/4.0/>).

## 1. Introduction

The coplanar waveguide (CPW) has been proved to be one of the most popular planar transmission lines in microwave and millimeter-wave applications. Due to the coplanar structure of the CPW, where the signal line and the two ground planes are placed on the same side of the substrate, surface mount and active devices can be easily integrated with the CPW transmission line [1–6]. In spite of the wide use of printed planar circuits in microwave and millimeter-wave systems, metallic waveguides still play an essential role in various components such as high-gain antennas [7], filters [8], diplexers, amplifiers [9] and so on. In some microwave and millimeter-wave systems, it is necessary to apply both CPW and rectangular waveguide; thus, developing a high-performance transition between them is needed. Over the last few decades, various CPW-to-waveguide transitions have been reported in the literatures [10–16]. Based on the relative position between the waveguide and the coplanar waveguide, the designs can be classified into two distinct types: in-line and right-angle transitions. More precisely, the main axes of the in-line configurations are collinear, while the right-angle configurations are perpendicular.

Several approaches have been proposed to improve the performance of in-line transition between the CPW and rectangular waveguide in [10–13]. As is reported in [10], a CPW-to-rectangular-waveguide transition can be achieved by using a tapered fin-line, but this suffers from an electrically large substrate size. In [11], the transition of CPW to RWG was achieved on a high-permittivity sapphire substrate. However, the above-mentioned structures in [11–13] need air-bridges to enhance their performance. At the same time, right-angle transitions between CPWs and rectangular waveguides have also been widely studied [14–16]. A compact CPW-to-RWG transition can be accomplished by exploiting slot antenna [14], while the bandwidth needs to be further expanded. A four-step Chebyshev impedance transformer and a matching stub over the quartz CPW are employed in the

transition of CPW-to-RWG [15]. The structure increases the complexity of manufacturing, which makes the actual processing more difficult. Recently, the metal ridge was introduced to guide the signal from the rectangular waveguide to CPW with gap termination [16]. The metal ridge makes the fabrication complicated. Most of the previous works [12–16] were optimized for low-permittivity substrates. The transitions in [10,11] can be realized on a high-dielectric-constant dielectric substrate, but the transition circuit occupies an electrically large area because of the tapered fin-line [10] and the relative bandwidth is merely 21.1% in [11].

In this letter, a broad CPW-to-RWG transition is proposed. By introducing a rectangular radiator etched with a semi-elliptic slot, the transition was achieved experimentally. The advantages of this design are as follows: (1) this transition can be realized on both high- and low permittivity materials ( $\epsilon_r = 10.2$  and  $\epsilon_r = 2.22$ ); (2) the improved bandwidths of 44.7% and 47.6% have been achieved, respectively; (3) the circuit structure is simple, which reduces the manufacturing difficulty in manufacture processing.

## 2. Configuration and Design

The structure of the proposed transition between CPW and rectangular waveguide, which uses an RT/Duroid 6010 substrate, is shown in Figure 1. The configuration of the transition consists of coplanar waveguide (CPW), a rectangular radiator etched with a half-Elliptic slot and a rectangular waveguide. The transition structure is symmetrical about the z-axis and the CPW is printed on an RT/Duroid 6010 substrate with a relative dielectric constant of 10.2, a loss tangent of 0.0023 and thickness of 0.635 mm. The view of planar circuit for CPW-to-RGW transition ( $\epsilon_r = 10.2$ ) is shown in Figure 2a. A radiator is connected to the coplanar waveguide's central conductor for energy coupling. The rectangular waveguide used in this design is WR-90, a standard waveguide with dimensions of  $22.86 \times 10.16$  mm, which will ensure single  $TE_{10}$  mode propagation in the X-band. The CPW transmits quasi-TEM mode, and the impedance matching with the rectangular waveguide can be realized by adjusting the related parameters of the radiator.

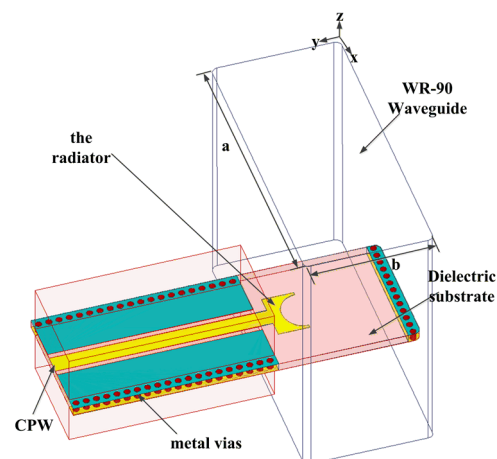
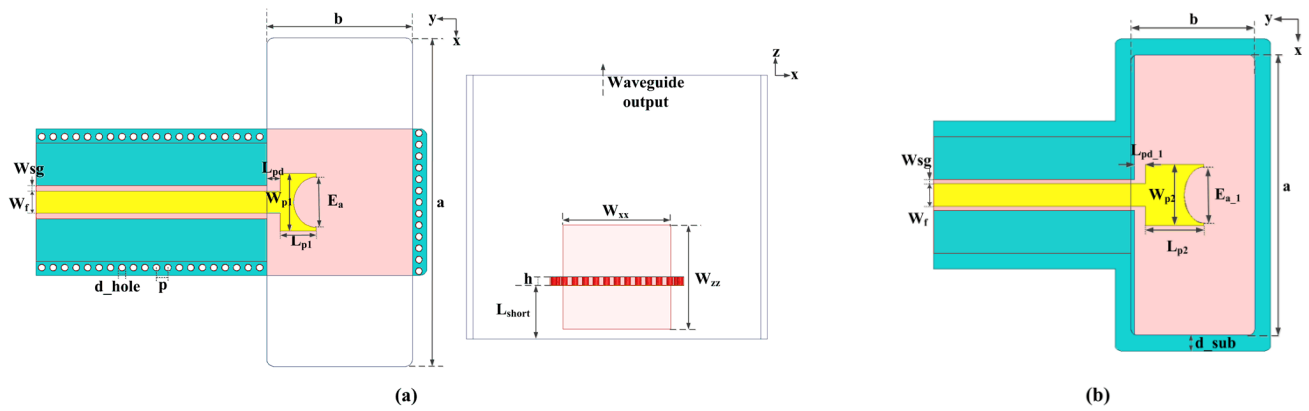


Figure 1. Configuration of proposed transition.

As shown in Figure 2a, the radiator is inserted from the broad wall of the waveguide, and is vertical with the z-axis. Note that the substrate embedded with the radiator is placed approximately one-quarter-wavelength away from the waveguide short plane, and shown with  $L_{\text{short}}$  in Figure 2a. The radiator used in this transition is formed by cutting a semi-elliptic slot in a rectangular patch. The etched semi-ellipse is arc-shaped, so the radiator used in this transition has a continuous change in distance from the wall of the waveguide. This can bring in continuously tunable electrical resonance lengths for fed-waves of different frequencies. In operation, the waveguide will work as a ground, and it will generate multiple resonances with the radiator. Additionally, two rows of metal

vias are placed in parallel on each ground plane of CPW. The role of the metal vias is to suppress energy leakage of the electromagnetic wave.



**Figure 2.** Layout of the proposed transitions: (a) the design with RT/Duroid 6010; (b) the design with RT/Duroid 5880.

All simulated and optimized processes of this proposed transition use a full-wave electromagnetic simulator. Table 1 lists some key parameters of the transition (the design with RT/Duroid 6010). Among them,  $W_{p1}$  and  $L_{p1}$  are the length of the rectangular sides,  $E_a$  is the major radius (in  $x$ -axis) of the half-ellipse, and ratio\_1 is the aspect ratio of the secondary radius to the major radius in the radiator structure.

**Table 1.** Structure parameters of the transition with RT/Duroid 6010 substrate (unit: mm).

$W_{p1}$	$L_{p1}$	$E_a$	ratio_1	$d_{hole}$	$p$	$W_f$
4	2.5	3.5	0.9	0.45	0.8	1.5
$W_{sg}$	$L_{pd}$	$W_{xx}$	$W_{zz}$	$L_{short}$	$a$	$b$
0.41	0.95	8.2	7.9	4.408	22.86	10.16

The structure of the proposed transition between CPW and a rectangular waveguide which uses RT/Duroid 5880 substrate is similar to the former structure shown in Figure 1. The RT/Duroid 5880 is a substrate with a relative dielectric constant of 2.22, loss tangent of 0.0009 and thickness of 0.787 mm. When switching from RT/Duroid 6010 substrate to RT/Duroid 5880 substrate, there is no need to redesign the overall transition. A broadband performance can be achieved by tuning the related parameters of the radiator. The parameters used to describe this transition are shown in Figure 2b. Table 2 lists some key parameters of the transition (the design with RT/Duroid 5880).

**Table 2.** Structure parameters of the transition with RT/Duroid 5880 substrate (unit: mm).

$W_{p2}$	$L_{p2}$	$E_{a_1}$	ratio_2	$W_f$	$W_{sg}$
4	2.5	3.5	0.7	1.5	0.41
$L_{pd_1}$	$W_{xx}$	$W_{zz}$	$L_{short}$	$a$	$b$
0.95	8.2	7.9	4.408	22.86	10.16

The proposed structure uses a rectangular radiator etched with a semi-elliptical slot to realize the direct transition between the rectangular waveguide  $TE_{10}$  mode to the CPW quasi-TEM mode. To demonstrate that a better return loss ( $S_{11}$ ) can be achieved by applying a rectangular radiator etched with a semi-elliptical slot in this paper, three different transitions (the transitions in this paper, the transition with semicircle radiator and the one with rectangular radiator) were simulated separately, and the  $S_{11}$  comparison of back-to-back transitions were shown in Figure 3. Then, it is necessary to study the effect of radiator

parameters on the performance of this proposed transition. Taking the transition with RT/Duroid 6010 as example, the S-parameters against frequency for different values of the ratio<sub>1</sub> in the radiator is shown in Figure 4. As can be seen from Figure 4, a new resonance point appears at 10.5 GHz around when ratio<sub>1</sub> = 0.9. At the same time, the bandwidth is slightly wider than the one choosing other two values.

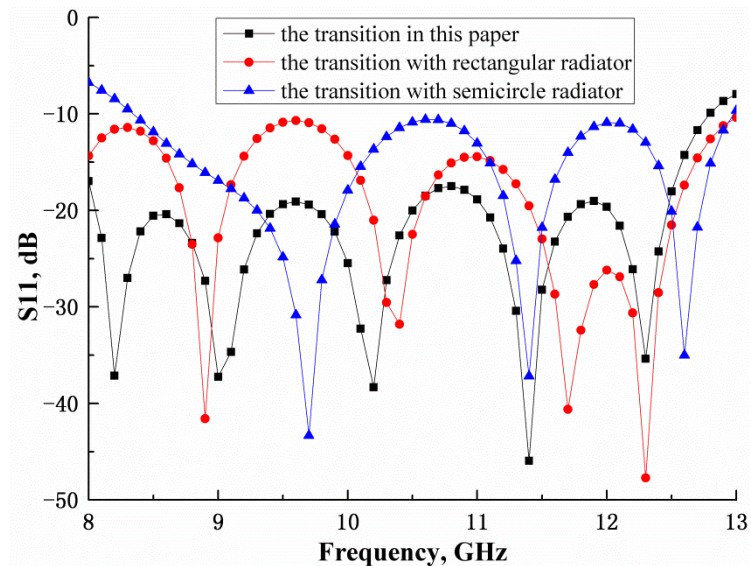


Figure 3. The S-parameter comparison of back-to-back transitions with different radiators.

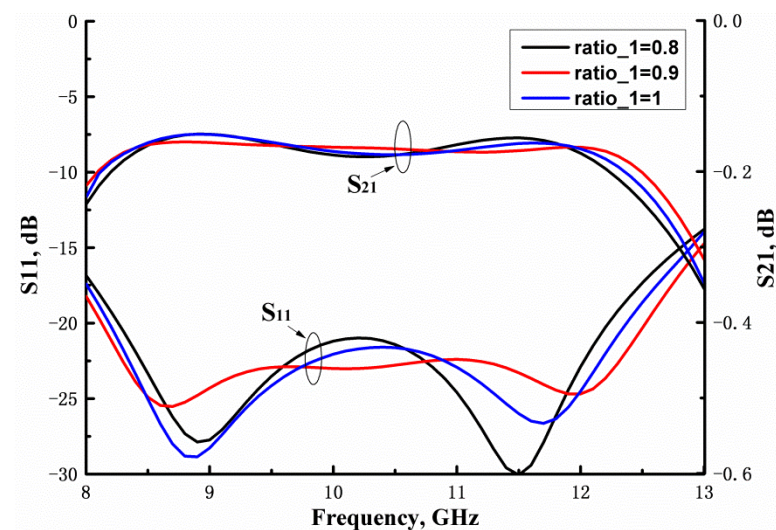


Figure 4. Simulated S-parameters of waveguide-to-CPW with varying parameters.

### 3. Measurement

To experimentally validate the simulation results and test the performance of the proposed transition, two back-to-back configurations were designed and fabricated to form the test circuit. The photos of the fabricated prototype are shown in Figure 5. The S-parameters of the fabricated transition were measured with a vector network analyzer after the equipment was calibrated by using WR-90 waveguide calibration kit. Moreover, a test fixture is adopted to measure the transmission coefficient of the transition. The measured results along with simulated results for comparison are also shown in Figure 6a ( $\epsilon_r = 10.2$ ) and Figure 6b ( $\epsilon_r = 2.22$ ).



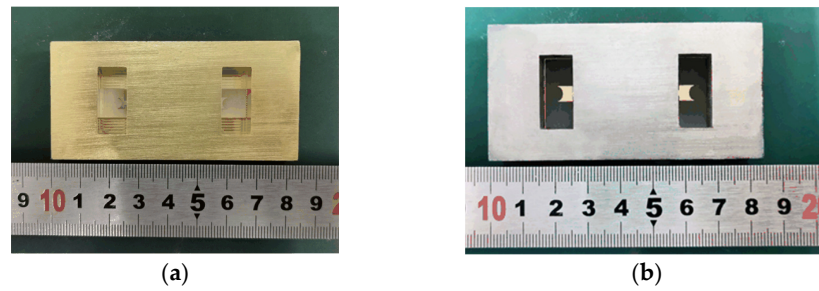


Figure 5. Photos of the fabricated prototype: (a) ( $\epsilon_r = 10.2$ ); (b) ( $\epsilon_r = 2.22$ ).

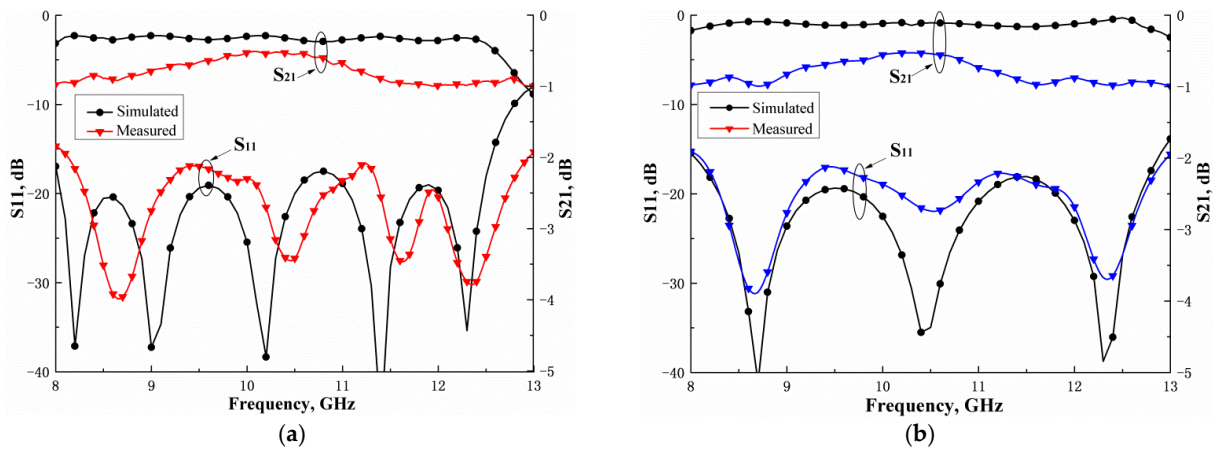


Figure 6. Measured and simulated results for the back-to-back transition: (a) ( $\epsilon_r = 10.2$ ); (b) ( $\epsilon_r = 2.22$ ).

The results show that the operation bandwidths of the two back-to-back transitions cover the entire X-band, meanwhile 44.7% ( $\epsilon_r = 10.2$ ) and 47.6% ( $\epsilon_r = 2.22$ ) of the broadband are achieved with low loss and good impedance matching, respectively. As can be seen from Figure 6, the measurement and simulation results are in good agreement. The slight deviation is attributed to the fabrication tolerance and inaccuracy of assembly.

Table 3 summarizes the performance comparison between this proposed waveguide-to-CPW transition and some previously reported works. There are two kinds of transitions sorted by the propagation direction, which are in-line [10,12,13] and right-angle [14–16]. The transitions proposed in this letter are designed for the application of right-angle systems. Compared with the transitions in [10,12–16], it is obvious that the proposed transition is suitable for both high- and low-dielectric-constant dielectric circuit substrate, and can achieve a wider operational bandwidth simultaneously.

Table 3. Comparison of waveguide-to-CPW transitions.

	Frquency Band	BW (GHz)	Relative BW	RL (dB)	IL (dB)	Structure	Fabrication Substrate (Permittivity)	Transition Direction
[10]	X	8.2–12.4	40.78%	>16	<0.4	back-to-back	NA/(2.33)	In-line
		8.2–12.4	40.78%	>10	<1		NA/(10.8)	
[12]	X	8.2–12.4	40.78%	>13.24	<0.43	single	RT/Duroid 5880 (2.22)	In-line
[13]	X	8.6–12.75	39.5%	>20	<1	single	RT/Duroid 5880 (2.22)	In-line
[14]	X	9.45–12.9	30.9%	>10	<1	back-to-back	RT/Duroid 5880 (2.22)	Right-angle
[15]	W	80–109	31.5%	>10	<1.2	back-to-back	Quartz (3.78)	Right-angle
[16]	U	40–60	40%	>12	<2.6	back-to-back	RT/Duroid 6002 (2.94)	Right-angle
This work	X	8–13	47.6%	>15	<0.95	back-to-back	RT/Duroid 5880 (2.22)	Right-angle
		8–12.58	44.7%	>15	<1		RT/Duroid 6010 (10.2)	

#### 4. Conclusions

A novel wideband and compact design of a right-angle coplanar waveguide to a rectangular waveguide transition for X-band application is introduced in this article. This design can be obtained with low- and high-permittivity materials ( $\epsilon_r = 10.2$  and 2.22).

Measurement results show that the two back-to-back transitions exhibit the impedance bandwidth of 44.7% ( $\epsilon_r = 10.2$ ) and 47.6% ( $\epsilon_r = 2.22$ ) for  $S_{11} < -15$  dB, respectively. The measurement results of the back-to-back configurations are in reasonable agreement with the simulation results, which shows that this transition structure can be used in a variety of microwave applications.

**Author Contributions:** Conceptualization, Y.Z. and J.D.; methodology, K.X.; software, F.Y.; validation, F.Y., X.F. and K.X.; formal analysis, F.Y.; investigation, X.F.; resources, J.D.; data curation, Y.Z.; writing—original draft preparation, Y.Z.; writing—review and editing, J.D.; visualization, X.F.; supervision, K.X.; project administration, J.D.; funding acquisition, J.D. All authors have read and agreed to the published version of the manuscript.

**Funding:** This research was supported by China Postdoctoral Science Foundation under Grant 2018M633666, Natural Science Foundation of Hunan Province under Grant 2019JJ50392, Opening fund of State Key Laboratory of Millimeter Waves under Grant K202116, and Scientific Research Fund of Hunan Provincial Education Department under Grant 17B160. Hunan College Students' innovation and entrepreneurship training program (2020-2163).

**Institutional Review Board Statement:** Not applicable.

**Informed Consent Statement:** Not applicable.

**Data Availability Statement:** Not applicable.

**Acknowledgments:** Thanks to the State Key Laboratory of Millimeter Waves, Southeast University Nanjing for help with this project.

**Conflicts of Interest:** The authors declare no conflict of interest.

## References

1. Simons, R.A. *Coplanar Waveguide Circuits, Components and Systems*; John Wiley & Sons: New York, NY, USA, 2001.
2. Dong, J.; Yang, T.; Liu, Y.; Yang, Z.; Zhou, Y.H. Broadband Rectangular Waveguide to GCPW Transition. *Prog. Electromagn. Res. Lett.* **2014**, *46*, 107–112. [[CrossRef](#)]
3. Lin, M.T.; Liu, P.G.; Gao, Y.; Liu, J.B. Improved SIW Corrugated Technique with Grounded Coplanar Waveguide Transition. *IEEE Antennas Wirel. Propag. Lett.* **2018**, *17*, 978–982. [[CrossRef](#)]
4. Wong, K.L.; Chang, H.J.; Wang, C.Y.; Wang, S.Y. Very-Low-Profile Grounded Coplanar Waveguide-Fed Dual-Band WLAN Slot Antenna for On-Body Antenna Application. *IEEE Antennas Wirel. Propag. Lett.* **2020**, *19*, 213–217. [[CrossRef](#)]
5. Lalbakhsh, A.; Mohamadpour, G.; Roshani, S.; Ami, M.; Roshani, S.; Sayem, A.S.M.; Koziel, S. Design of a Compact Planar Transmission Line for Miniaturized Rat-Race Coupler with Harmonics Suppression. *IEEE Access* **2021**, *9*, 129207–129217.
6. Xu, K.D.; Xia, S.P.; Jiang, Y.N.; Guo, Y.J.; Liu, Y.Q.; Wu, R.; Cui, J.L.; Chen, Q. Compact millimeter-wave on-chip dual-band bandpass filter in 0.15- $\mu\text{m}$  GaAs Technology. *IEEE J. Electron. Devices Soc.* **2022**, *10*, 152–156.
7. Elliott, R.S. An Improved Design Procedure for Small Arrays of Shunt Slots. *IEEE Trans. Antennas Propagat.* **1983**, *31*, 48–53. [[CrossRef](#)]
8. Wu, Q.; Zhu, F.; Yang, Y.; Shi, X. An Effective Approach to Suppressing the Spurious Mode in Rectangular Waveguide Filters. *IEEE Microw. Wirel. Compon. Lett.* **2019**, *29*, 703–705. [[CrossRef](#)]
9. Roshani, S. Two-section Impedance Transformer Design and Modeling for Power Amplifier Applications. *Appl. Comput. Electromagn. Soc. J. (ACES)* **2017**, *32*, 1042–1047.
10. Möttönen, V.S. Wideband Coplanar Waveguide-to-Rectangular Waveguide Transition using Fin-Line Taper. *IEEE Microw. Wirel. Compon. Lett.* **2005**, *15*, 119–121. [[CrossRef](#)]
11. Moon, S.W.; Lee, S.J.; Han, M.; Rhee, J.K.; Kim, S.D. Transition of 94-GHz Coplanar Waveguide to Rectangular Waveguide on Flip-Chip Bonding Compatible Substrate. *Microw. Opt. Technol. Lett.* **2011**, *53*, 1694–1697. [[CrossRef](#)]
12. Fang, R.Y.; Wang, C.L. Miniaturized Coplanar Waveguide to Rectangular Waveguide Transition Using Inductance-Compensated Slotline. *IEEE Trans. Compon. Packag. Manuf. Technol.* **2012**, *2*, 1666–1671. [[CrossRef](#)]
13. Wang, S.H.; Chang, C.C.; Lee, Y.C.; Wang, C.L. Compact and Broadband CPW-to-RWG Transition Using Stub Resonators. *IEEE Trans. Microw. Theory Tech.* **2016**, *64*, 3198–3207. [[CrossRef](#)]
14. Fang, R.Y.; Wang, C.T.; Wang, C.L. Coplanar-to-Rectangular Waveguide Transitions Using Slot Antennas. *IEEE Trans. Compon. Packag. Manuf. Technol.* **2011**, *1*, 681–688. [[CrossRef](#)]
15. Wang, C.; Yao, Y.; Wang, J.; Cheng, X.H.; Yu, J.S.; Chen, X.D. A Wideband Contactless CPW to W-Band Waveguide Transition. *IEEE Microw. Wirel. Compon. Lett.* **2019**, *29*, 706–709. [[CrossRef](#)]
16. Dong, Y.F.; Zhurbenko, V.; Johansen, T.K. A U-Band Rectangular Waveguide-to-Coplanar waveguide Transition Using Metal Ridge. In Proceedings of the 50th European Microwave Conference, Utrecht, The Netherlands, 2 February 2021.